

# Three-jet electrospinning using a flat spinneret

Feng-Lei Zhou · Rong-Hua Gong · Isaac Porat

Received: 20 April 2009 / Accepted: 21 July 2009 / Published online: 4 August 2009  
© Springer Science+Business Media, LLC 2009

**Abstract** Electrospinning is a simple but highly versatile technology to produce nanofibers from solutions or melts mostly of polymers using electrostatic forces. A primary challenge facing electrospinning is its low productivity mainly limited by flow rate. In this work, a custom-made three-hole spinneret instead of conventional needles was adopted to enhance the flow rate of electrospinning. Three-jet formation, nanofiber deposition, nanofiber morphology and size were characterized by digital camera and scanning electron microscopy (SEM) as the effects of several governing parameters in electrospinning, including applied voltage from 19.8 to 21.0 kV, working distance from 15.2 to 16.8 cm and flow rate from 6.0 to 9.0 mL/h. It was found that three simultaneous stable jets were ejected from the three-hole spinneret under suitable operating conditions. Moreover, it was found that the fibers collected from the jets from each hole deposited separately in circular spots on a stationary collector. The resultant fibers mostly have an average diameter of less than 300 nm. It has been proved that simple holes on a flat surface can be used to electrospin nanofibers. The three-hole spinneret produces nanofibers at flow rates greater than that in single needle electrospinning. Flow rate has the potential to be easily scaled up by increasing the spinneret diameter and the number of holes.

## Introduction

Electrospinning is a process capable of producing various assemblies of continuous nanofibers with controlled morphology and size from polymer solutions or melts in high electric fields. In most published works devoted to investigate electrospinning, the authors have used experimental lab-scale setups equipped with a syringe needle with a fixed diameter of 0.3–1.0 mm [1]. The flow rate in single needle electrospinning process is typically 1.0–5.0 mL/h [2]. For most applications of nanofibers, such low flow rate puts severe limits to the use of single needle electrospinning unless a high number of needles are simultaneously operated. Various approaches based on modifying spinnerets have been reported to enhance the flow rate in electrospinning process in the last few years [3]. These methods can be generally divided into two categories: multi-needle and needleless electrospinning. A common characteristic of multi-needle electrospinning is the employment of needle-like shapes to anchor the electrified conical menisci. Multi-needle electrospinning, however, is subject to several disadvantages, such as complex design and potential clogging. In the case of needleless electrospinning, multiple jets have been demonstrated to be ejected from free surface of polymer solutions, instead of needles [4]. Though this method eliminates the high possibility of clogging, loose control of the multi-jet formation leads to difficulties in obtaining nanofibers with desired morphology and size. Recently, holes on flat metallic or plastic surfaces were successfully used in electrospinning process in steady cone-jet mode for fabrication of ultrafine particles [5–7]. For example, it was observed that the stable cone-jet is formed at the rim of the hole drilled on a hydrophobic plate [6]. Our preceding work has revealed that smooth

F.-L. Zhou (✉) · R.-H. Gong · I. Porat  
Department of Textiles & Paper, School of Materials,  
The University of Manchester, Manchester M60 1QD, UK  
e-mail: fenglei.zhou@postgrad.manchester.ac.uk

nanofibers can be produced by single hole flat spinneret electrospinning (FSE) [8].

In the present study, a three-hole spinneret was made to study the potential to increase the flow rate in electrospinning. Advantages of using holes instead of multi-needle include ease of fabrication, simple design, low cost of manufacturing and clogging probability. The jets formation and deposition in the three-jet electrospinning process have been investigated. The morphology and size of resultant nanofibers produced under various process parameters were presented.

## Experimental

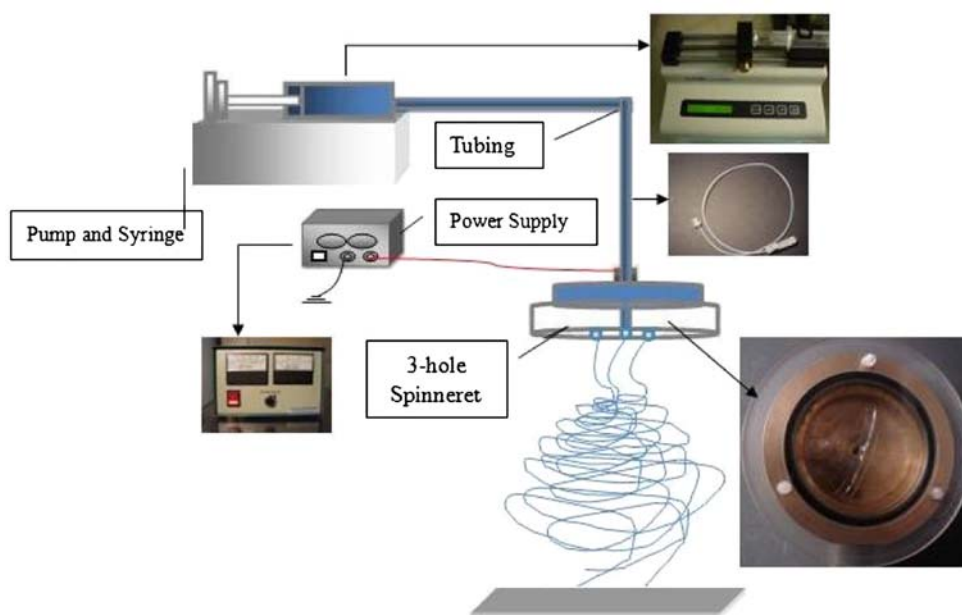
### Materials

Polyethylene oxide (PEO), with an average viscosity molecular weight ( $M_v$ ) of  $9 \times 10^5$  (g/mol), was obtained from Sigma-Aldrich, UK, and used as received, while distilled water was prepared using double distillation (Fistream-Cyclon, UK). PEO powder was dissolved in distilled water into solution with 6 wt% concentration at ambient temperature and about 72 h were allowed for the complete dissolution during which the solution was placed on a rotating magnetic mixer (Kika Labortechnik RCT Basic Heater/Stirrer) for gentle mixing.

### Three-hole electrospinning setup

The schematics and the basic apparatus of three-hole electrospinning process are shown in Fig. 1. The electrospinning apparatus consists of a flat spinneret connected to

**Fig. 1** Schematic and the apparatus of electrospinning from three-hole on flat surface for fabrication of nanofibers (not to scale)



the positive electrode of a high voltage power supply (ES30P-20W, Gamma High Voltage Research Inc., Ormond Beach, FL) that is capable of generating DC voltages up to 30 kV, a pump system (KDS 100, kdScientific) and a grounded aluminium plate.

The three-hole spinneret comprises a cylindrical cap, with a flat end surface, on which three holes with 10 mm spacing are drilled (Fig. 2). Polycarbonate was reported by Tang et al. [9] to fabricate an emitter array for the generation of multiple electrospays. Polycarbonate, therefore, was chosen to build the cylindrical cap. The cylindrical cap closes a hollow cylindrical metallic cavity, served as a solution reservoir allowing a uniform flow to each hole. For varying the hole number or array, only the cylindrical cap needs to be changed. A metallic inlet behind the reservoir provides solution feeding, but also electrical connection to

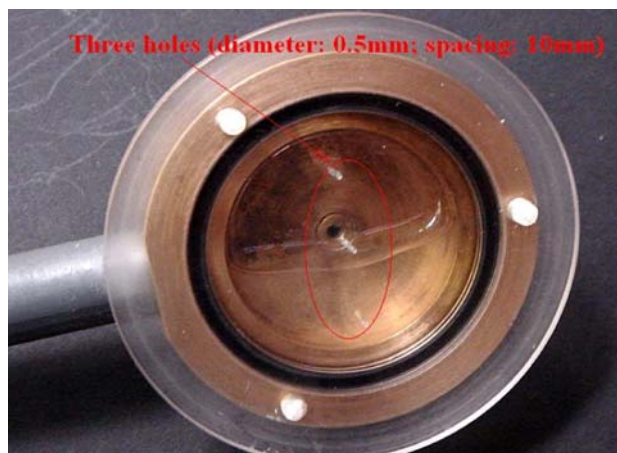


**Fig. 2** Photograph of three-hole spinneret with linear array

**Table 1** Experimental parameters

Experimental no.	Process parameters		
	Applied voltage (kV)	Flow rate (mL/h)	Working distance (cm)
1	19.8	7.5	16.0
2	20.4	7.5	16.0
3	21.0	7.5	16.0
4	20.4	6.0	16.0
5	20.4	9.0	16.0
6	20.4	7.5	15.2
7	20.4	7.5	16.8

the solution. In order to commence electrospinning, a 20 mL glass syringe was placed on the pump; the pump was turned on to supply a continuous flow of solution and a high voltage was applied. During electrospinning, PEO solution passed through Teflon<sup>®</sup> tubing with two Kel-F<sup>®</sup> hubs (18 gauge  $\times$  50 cm, Hamilton) to the spinneret fixed on a wooden frame at adjustable distance of 5.0–30.0 cm above the aluminium plain collector. In general, electrospinning was performed for around 18 min and PEO fibers were collected on aluminium foil placed on the grounded collector. Electrospinning trials were performed to determine the processing window of PEO-water solution with 6 wt% concentration. To evaluate the effects of process parameters, seven groups of experimental designs within the processing window were formulated in a way that provides relatively stable three-jet process (Table 1). All experiments were done under ambient conditions.

#### Characterization of nanofiber morphology and deposition pattern

SEM images with the magnifications of 2500 $\times$  and 10000 $\times$ , respectively, were used for the fibers from each hole and at least 30 measurements were conducted from each of the SEM images with 10000 $\times$  magnification, so that altogether 90 separate measurements were conducted using NIH ImageJ software from each sample. Thus, totally 270 separate measurements for each group are used to determine the fiber average diameter. The three-jet electrospinning process and the deposition patterns of nanofibers were registered by a Sony DSC-T5 digital camera.

## Results and discussion

The multi-jet formation, the morphology and the diameter of PEO nanofibers could be adjusted by controlling various operating parameters including applied voltage, flow rate and working distance in electrospinning process.

### Multi-jet formation

In single needle electrospinning process, the jet formation strongly depends on a dynamic balance of surface tension, electrostatic, Coulombic, air drag, and gravitational forces [10, 11]. It has been found in single needle electrospinning process that the shape of the initiating droplet on the syringe needle tip can be changed by applied voltage, flow rate and solution viscosity [12, 13]. When the jet number is increased in electrospinning, one more Coulombic repulsion force between jets is involved, which causes more complex process.

#### Effects of applied voltage, working distance and flow rate

For 6 wt% PEO-water, when applied voltage was lower than 15.0 kV, no cone or jet was formed because the electrostatic field strength is not strong enough to overcome the surface tension. Then, applied voltage was increased until a cone-jet was fully formed on each hole. However, when applied voltage was higher than 21.9 kV, it was also hard to obtain stable three-jet electrospinning process. As a result, applied voltage in stable three-jet electrospinning can only be varied from 15.0 to 21.9 kV.

It has been observed that the variation in applied voltage significantly alters the shape of the initiating droplet. At the applied voltages of 19.8, 20.4 and 21.0 kV, three conic droplets remained suspended at the exit of the holes, and three jets originated from the tip of three cones, respectively. At a voltage of 19.8 kV, however, it was observed that PEO solution dripping occurred to the pendant droplet on a side hole. The solution dripping immediately deteriorated the three-jet process and also reduced the size of the droplet, which affected the fiber morphology and size. When PEO solution was again accumulating on the side hole surface, the three-jet process appeared again. At 21.0 kV the volume of three droplets greatly decreased, and the diameter of each droplet was still much larger than the hole size. At 21.9 kV three jets appeared to be initiated directly from the holes without externally visible droplets and with a further increase in voltage, the jets disappeared. Although three holes in an array all have the same potential, they may not experience the same electric field due to end effects [6, 14–16]. Thus, the cones of the holes near the edge of the array are deformed and asymmetric. Similarly, an increase in distance (decrease in electric field strength) increases the volume of the droplets. Decreasing droplet volume due to the higher applied voltage or shorter working distance can be easily explained since higher electric field causes the jet velocity to increase and thus the solution to be removed from the hole surface more quickly. The droplets suspended at the surface of the spinneret were

larger with a higher feeding rate when all other variables (applied voltage, working distance) were held constant. Increasing droplets can also be easily explained since the rate of solution delivery to the holes needed to maintain the conical shapes of the surface increases at higher flow rate. However, higher flow rates can cause solution dripping, which usually destroys the web structure.

### Deposition of three jets

In the single jet electrospinning process, nanofibers are usually deposited on a grounded plate collector as a relatively uniform circular nonwoven web due to bending instabilities. In multi-needle electrospinning process with linear array, however, the nanofiber deposition on the fabrics was found to be somewhat inconsistent, which was caused by the repulsion of the jets [14, 17, 18]. This effect was found to be reduced by the introduction of more jets, for example, 2D matrices jet which leads to uniformity of the produced non-woven mat [17].

In the current three-hole process, it was observed that the mutually repulsing electrified jet underwent bending instabilities characteristic of single-jet electrospinning, which results in three circular but separated spots of nanofibers, as shown in Fig. 3. The nanofiber webs

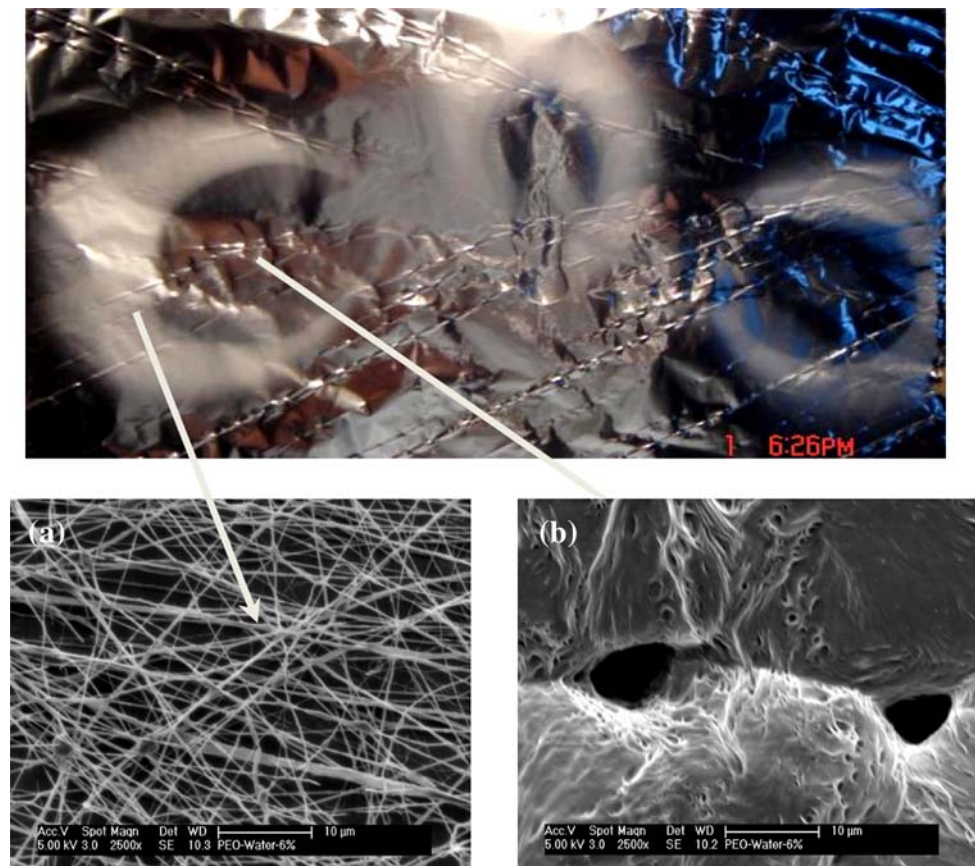
produced in each trial are visible as three white circles on aluminium foil on the grounded collector. However, the deposition areas of the two jets on the edge are apparently larger than that of the central jet. It can be easily explained by the fact that the envelope cone of the central jet along the line on which the holes are located is squeezed [17]. Each deposited fiber web is obviously different in the outer and inner regions. It was further revealed by SEM images that the outer and inner regions are composed of PEO nanofibers and PEO film, respectively (Fig. 3). The non-fibrous region was formed by the PEO jets, which reached the aluminium foil without being sufficiently stretched by the electric field and/or insufficient solvent evaporation. When working distance was increased to 16.8 cm, the ratio of the fibrous region to the film region in three spots greatly increased. Moreover, the stationary fiber collector may also contribute the formation of the dual morphology on one deposition [19].

### Morphology and diameter

#### Effects of applied voltage

Applied voltage influences the jet initiation, flight and fiber deposition, all of which are closely correlated with the size

**Fig. 3** SEM Images of **a** the inner region and **b** outer region of one deposition area in three-jet electrospinning process (from experimental No. 5 in Table 1)





and morphology of the resultant nanofibers. Applied voltage, therefore, is often considered the most essential parameter in electrospinning [20]. For PEO-water solution of 6 wt%, at a flow rate of 7.5 mL/h and a working distance of 16.0 cm, the morphology of PEO nanofibers obtained at applied voltages of 19.8, 20.4 and 21.0 kV are

shown in Fig. 4a–c. The nanofibers produced under these conditions have a cylindrical morphology with few bead defects present. As discussed in the multi-jet formation, the shape of the initiating droplet at the hole exit changes with the applied voltage and the resulting fiber diameter sharply changes accordingly. In this three-hole process, we

**Fig. 4** SEM micrographs and size distributions of PEO nanofibers produced at various applied voltages: **a** 19.8 kV, **b** 20.4 kV, and **c** 21.0 kV; working distances: **d** 15.2 cm and **e** 16.8 cm; flow rates: **f** 6.0 mL/h and **g** 9.0 mL/h

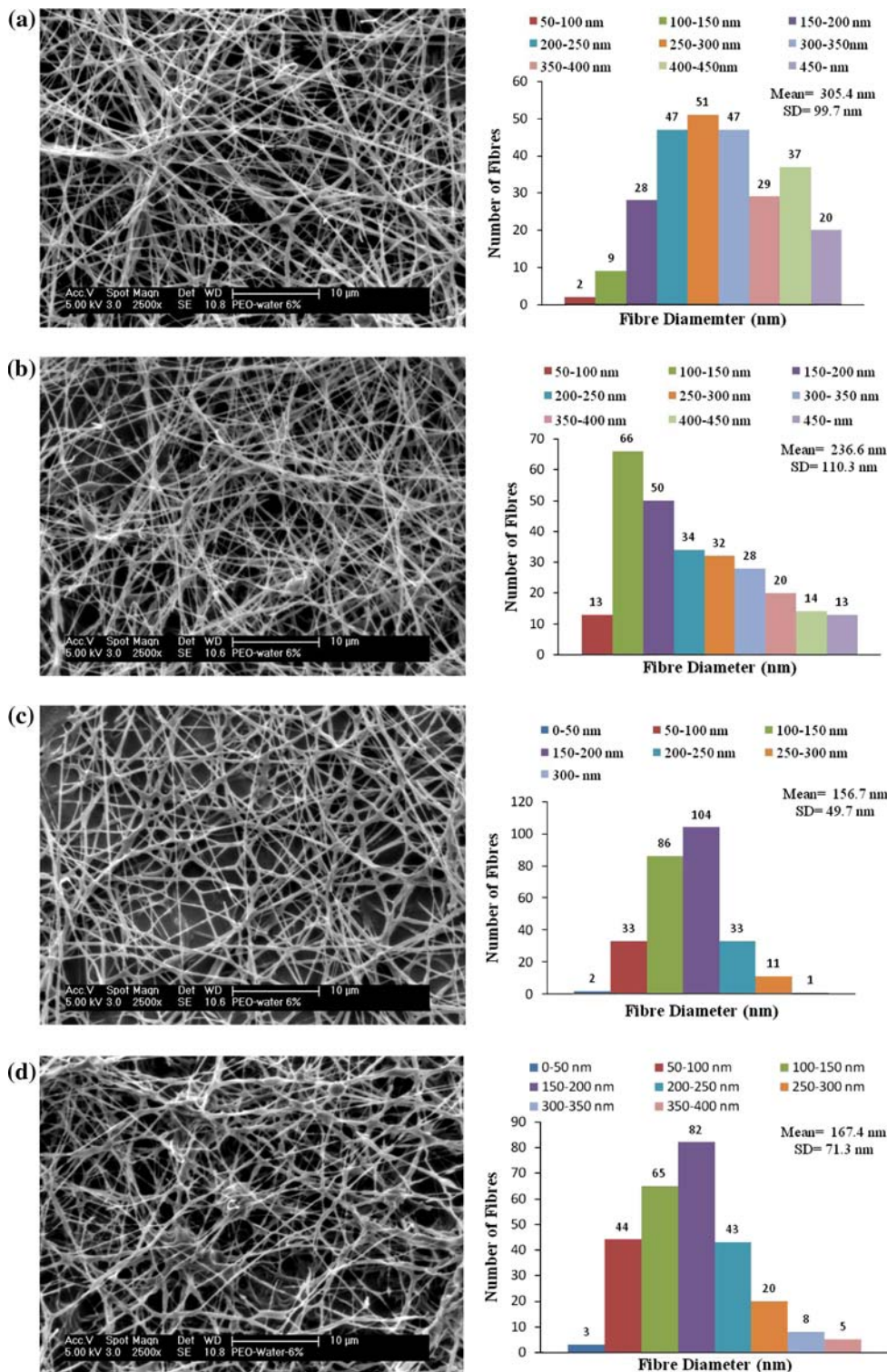
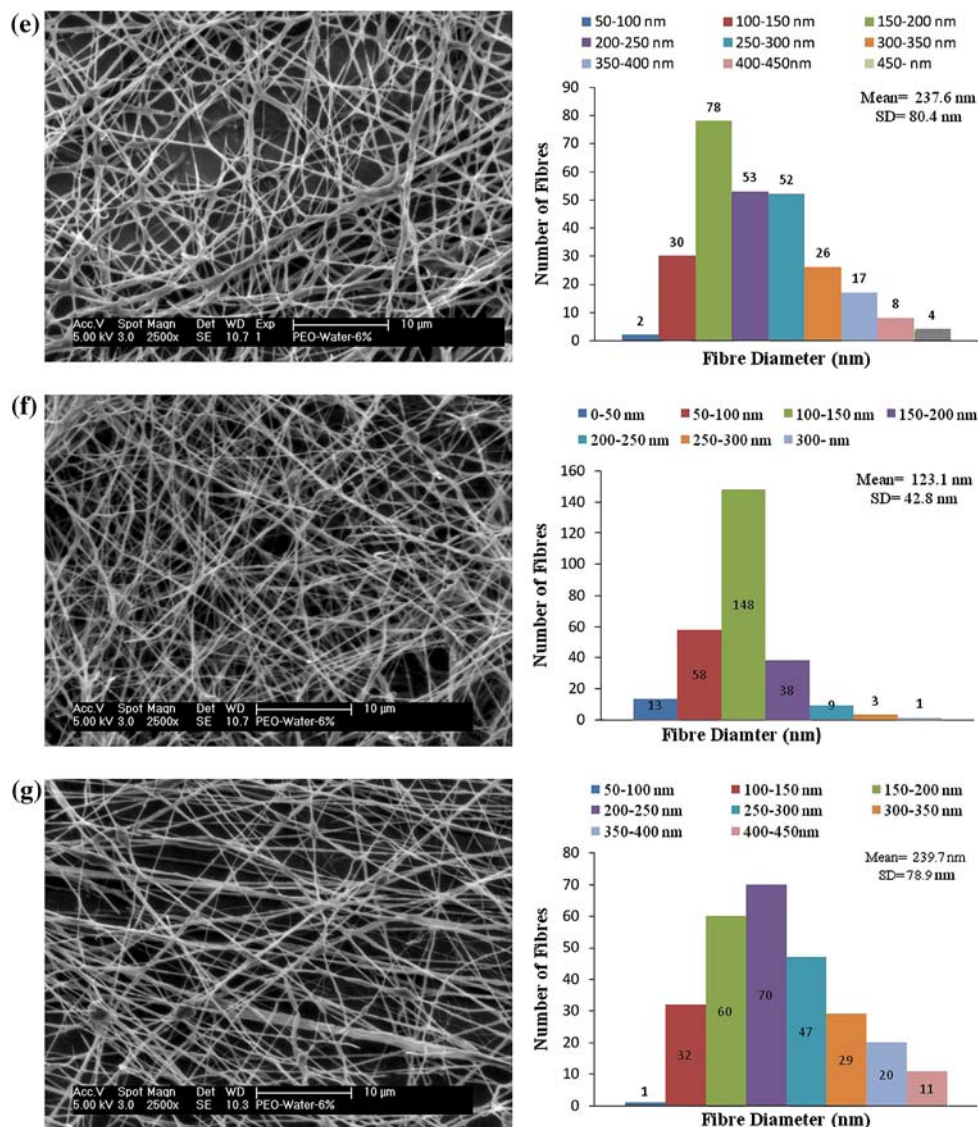


Fig. 4 continued



obtained a monotonic dependence curve between the fiber average diameter and the applied voltage. At fixed flow rate and working distance, the average diameter decreases by around 50% from 305.4 to 156.7 nm with the increasing applied voltage. Decreasing fiber diameter due to the higher voltage can be easily explained, since higher voltage induces higher electrostatic forces on the jet, and higher repulsive forces favour the formation of the thinner fibers. The diameter distribution became narrower with the increasing applied voltage if the bead defects were not included for the calculation. Similar results have been reported in previous single needle electrospinning [21–24]. Further image analysis revealed that PEO nanofibers obtained at 20.4 and 21.0 kV have a unimodal size distribution and, however, the fibers produced at 19.8 kV exhibit a bimodal distribution. The primary and secondary fibers in

the distribution have average diameters of about 275.0 and 425.0 nm, respectively. The secondary population of fibers have diameters about 1.5 times that of the primary fibers and make up about 30% of the total number of fibers. Such bimodal distributions have been also reported previously in many systems [13, 25, 26]. Two potential explanations have been suggested for the formation of bimodal size distributions in the fibers obtained on the collector: (a) fiber jets emerging from smaller satellite drops and (b) repeated splaying of the fiber jets. It is conceivable that the explanations provided above for the formation of secondary fibers with lower diameter may still be applicable; however, the formation of fibers with larger diameter has to be explained by yet another mechanism. It is likely that the secondary population observed in the distribution of the electrospun PEO fibers is formed due to solution dripping [27].

### Effect of working distance

In single needle electrospinning, working distance is also considered as a key factor that affects the diameter of the resulting nanofibers and the relationship can be quantitatively described as a power law regression with slope from  $-2$  to  $-21$  [28]. However, it was also reported that working distance does not play a dominant influence on the jet and fiber diameter during electrospinning when point-to-plate electrode configuration was used [24]. In the 3-hole process, it was found that working distance is able to influence the morphology and the diameter of the resultant PEO fibers. Figure 4b, d–e shows SEM images of fibers electrospun from PEO solution under three different working distances. Beaded fibers were produced at working distance of 15.2 cm, where the remaining solvent in the jets did not have enough time to evaporate when they reached the collector. With further increase in working distance, relatively large amount of smooth electrospun fibers with larger diameters were collected. It was observed that there is a rapid increase in fiber diameter with the increase in collecting distance from 15.2 to 16.0 cm, followed by a slight increase at 16.8 cm, where more smooth fibers were produced. Increasing diameter due to higher working distance can be easily explained, since higher working distance leads to weaker electrostatic forces on the jet and reduces stretching. The slight increase in fiber diameter may be explained by solution dripping, which occurred when the working distance was set to be 16.8 cm or higher.

### Effect of flow rate

Flow rate is one of the key parameters that determines the final jet diameter during single jet electrospinning process [29]. Theoretically, stable three-jet FSE process can be accomplished by simultaneously adjusting applied voltage and flow rate after the onset of electrospinning is achieved. Practically, this is very difficult to control as a high flow rate would result in excessive solution plummeting to the collector, disrupting the delicate three-jet process, while a low flow rate would cause the pendant droplet to shrink quickly and terminate the three-jet process. Though no investigation was reported on the influences of flow rate in multi-jet electrospinning process, it was observed that flow rate can influence the multi-jet electrospinning performance like the onset applied voltage, spray current, jet diameter and droplet size [30, 31]. For example, higher flow rate leads to larger jet diameter and droplet size. It was also pointed out that an appropriate flow rate selection should be based on the sample availability and operating conditions. At a fixed applied voltage and working distance, there exists a processing window for the flow rate to

form stable cone-jet electrospinning. In this study, the total flow rate ranging from 6.0 to 9.0 mL/h (2.0–3.0 mL/h/hole) was used to achieve stable electrospinning process, when applied voltage and working distance were set 20.4 kV and 16.0 cm, respectively. The morphological structure slightly changes with the solution flow rate as shown in Fig. 4b, f–g. The average fiber diameter varies from 123.1 to 239.7 nm and the diameter distribution firstly increases then drop when flow rate is increased from 6.0 to 9.0 mL/h. It has been well demonstrated that fibers with larger diameter and broader diameter distribution are electrospun under higher flow rate in single jet electrospinning [12, 24, 32, 33]. This tendency is well understood because there is more volume of solution available to process under higher flow rate. Similarly, a lower flow rate of 6.0 mL/h narrows the distribution of fiber diameters, while a broad one is obtained at the flow rate of 7.5–9.0 mL/h. However, there is a much more significant rise of the average diameter when the flow rate changes from 6.0 to 7.5 mL/h, compared to the increase in the second change. This is most likely to be caused by solution dripping observed at the flow rate of 9.0 mL/h.

### Conclusions

We have presented some experimental evidence to electrospin nanofibers using a three-hole flat spinneret. These results show that nanofibers can be produced at higher flow rates than using single needle electrospinning. The design and setup of three-hole apparatus is relatively simple compared to the array of multi-needle electrospinning.

**Acknowledgements** Financial supports from the ORS award and School of Materials, The University of Manchester, are gratefully acknowledged. We would also like to thank Mr. S. Butt for the constructions of the electrospinning setup and flat spinnerets.

### References

1. Srivastava Y, Marquez M, Thorsen T (2007) *J Appl Polym Sci* 106:3171
2. Brown PJ, Stevens K (eds) (2007) *Nanofibers and nanotechnology in textiles*. Woodhead Publishing Limited, UK
3. Zhou FL, Gong RH, Porat I (2009) *Polym Int* 58:331
4. Yarin AL, Zussman E (2004) *Polymer* 45:2977
5. Lozano P, Martínez-Sánchez M, Lopez-Urdiales JM (2004) *J Colloid Interface Sci* 276:392
6. Bocanegra R et al (2005) *J Aerosol Sci* 36:1387
7. Byun D et al (2008) *Appl Phys Lett* 92:093507
8. Zhou FL, Gong RH, Porat I (2009) *Polym Eng Sci* (in production)
9. Tang K et al (2001) *Anal Chem* 73:1658
10. Ding B et al (2006) *Nanotechnology* 17:3685
11. Vaseashtaa A (2007) *Appl Phys Lett* 90:093115
12. Zong X et al (2002) *Polymer* 43:4403
13. Deitzel JM et al (2001) *Polymer* 42:261

14. Bowman J et al (2003) Mater Res Soc Symp 752:AA1.5.1
15. Hubacz AN, Marijnissen JCM (2003) J Aerosol Sci 34(Suppl 1): S1269
16. Quang TSB, Byun D, Lee S (2007) J Aerosol Sci 38:924
17. Theron SA et al (2005) Polymer 46:2889
18. Tomaszewski W, Szadkowski M (2005) Fibers Text East Eur 52:22
19. Varabhas JS, Chase GG, Reneker DH (2008) Polymer 49:4226
20. Subbiah T et al (2005) J Appl Polym Sci 96:557
21. Geng X, Kwon OH, Jang J (2005) Biomaterials 26:5427
22. Buchko CJ et al (1999) Polymer 40:7397
23. Megelski S et al (2002) Macromolecules 35:8456
24. Wang C, Hsu CH, Lin JH (2006) Macromolecules 39:7662
25. Demir MM et al (2002) Polymer 43:3303
26. Hsu CM, Shivkumar S (2004) Macromol Mater Eng 289:334
27. Heikkil P, Harlin A (2008) Eur Polym J 44:3067
28. Thompson CJ et al (2007) Polymer 48:6913
29. Fridrikh SV et al (2003) Phys Rev Lett 90:144502/1
30. Sen AK, Darabi JD, Knapp DR (2007) Microfluid Nanofluid 3:283
31. Duby MH et al (2006) J Aerosol Sci 37:306
32. Zeng J et al (2003) J Appl Polym Sci 89:1085
33. Li L, Hsieh YL (2005) Polymer 46:5133